Available online at www.sciencedirect.com
SCIENCE DIRECT
International Journal of Fatigue 28 (2006) 151–163
International Journal of Fatigue
www.elsevier.com/locate/ijfatigue

Stress concentration formula useful for all notch shape in a round bar (comparison between torsion, tension and bending)

Nao-Aki Noda*, Yasushi Takase

Mechanical Engineering Department, Kyushu Institute of Technology, 1-1, Sensui-cho, Tobata, Kitakyushu 804-8550, Japan

Received 3 December 2004; received in revised form 25 March 2005; accepted 4 April 2005
Available online 22 July 2005

Abstract

In this work, stress concentration factors (SCFs, K_t) of a round bar with a circular-arc or V-shaped notch are considered under torsion, tension and bending. First, for the limiting cases of deep and shallow notches, the body force method is used to calculate the SCFs; then, the formulas are obtained as K_{td} and K_{ts}. On the one hand, upon comparison between K_t and K_{td}, it is found that K_t is nearly equal to K_{td} if the notch is deep or blunt. On the other hand, if the notch is sharp or shallow, K_t is mainly controlled by K_{ts} and the notch depth. The notch shape is classified into several groups according to the notch radius and notch depth; then, the least squares method is applied for calculation of K_t/K_{td} and K_t/K_{ts}. Finally, a set of convenient formulas useful for any shape of notch in a round test specimen is proposed. The formulas yield SCFs with less than 1% error for any shape of notch. The effect of notch opening angle on the SCF is also considered for the limiting cases of deep and shallow notches.

Keywords: Fatigue; Stress concentration; Notch; Numerical analysis; Test specimen; Torsion; Tension; Bending

1. Introduction

The stress concentration factor of a round bar with a circumferential groove is mainly used in practice for the design of shafts (see Fig. 1). It is also important with respect to investigating fatigue strength and notch sensitivity of engineering materials. Since exact stress concentration factors are desirable for the research, the authors proposed accurate engineering formulas with less than 1% error useful for any dimensions of notch in a round bar under tension and bending [1,2]. However, the round bar specimen with a circumferential groove is also important in torsion problems.

In this study, therefore, stress concentration factors (SCFs) of a round bar with a circular-arc or V-shaped notch are considered under torsion, and then they are compared with the ones under tension and bending. In addition, the effect of notch opening angle upon the stress concentration is also discussed. It should be noted that the effect of notch dimensions on the stress concentration under torsion is different from the ones under tension and bending. Considering these differences, we will propose accurate engineering formulas useful for any dimensions of notches.

2. Effect of notch opening angle on the stress concentration factor for shallow and deep notches

In our previous studies, we fixed the notch opening angle $\omega = 60°$, and then proposed accurate formulas useful for any dimensions of notch in a round bar under tension and bending [1,2]. In this paper, first, we will consider the effect of the notch opening angle ω on the stress concentration factor under torsion, tension and bending. In previous research, Kikukawa-Satou [4] used strain gauges measurement, and investigated the stress concentration factor with varying a notch opening angle ω and depth of notch as $a/\rho = 1, 2, 4$ (see Fig. 1). Also, Nisitani [5,6] applied the body force method, and then studied the effect of a notch opening angle of a V-shaped notch semi-infinite plate when $t/\rho = 1, 2, 4, 8$. In addition, Murakami-Noda-Nisitani [7] examined the effect of the opening angle of the notch in a round bar under bending when $0.5 \geq 2\rho/D \geq 0.05$ in Fig. 1.

* Corresponding author. Tel./fax: +81 93 884 3124.
E-mail address: noda@mech.kyutech.ac.jp (N.-A. Noda).

0142-1123/$ - see front matter © 2005 Elsevier Ltd. All rights reserved.
doi:10.1016/j.ijfatigue.2005.04.015

Nomenclature

ρ	notch root radius
t	depth of notch
a	notch root radius at minimum section
d	diameter of minimum section, $d=2a$
D	diameter of maximum section
x	$x=a/\rho$, when $a/\rho<1.0$; $x=2-\rho/a$, when $\rho/a\leq 1.0$
λ	relative notch depth, $=2t/D$
ξ	$=\sqrt{t/\rho}$
η	$=\sqrt{\rho/t}$
ω	notch opening angle (degrees)
ω^*	$\omega/90$
K_t	stress concentration factor (SCF) based on the minimum section shown in Fig. 1(a)–(c)
$K_{t\mathrm{d}}$	SCF of deep notch, a limiting solution for $2t/D\to 1$
$K_{t\mathrm{E}}$	SCF of an elliptical hole in an infinite plate under uniform tension $(=1+2\sqrt{t/\rho})$
$K_{t\mathrm{H}}$	SCF of a deep hyperboloidal notch [3] $K_{t\mathrm{H}}=3(1+\sqrt{a/\rho+1})^2/4(1+2\sqrt{a/\rho+1})$
$K_{t\mathrm{s}}$	SCF of notch in a semi-infinite plate, a limiting solution for $2t/D\to 0$
$K_{t\mathrm{N}}^{m=2.6}$	SCF calculated by a modified Neuber formula with an exponent $m=2.6$
ν	Poisson's ratio $(=0.3)$
M_1	division number for circular-arc of notch
M_2	division number for straight-part of notch

However, usually, the effect of the opening angle varies depending on the sharpness and depth of the notch. In this study, therefore, we will examine the effect of the notch opening angle for the whole range of the notch dimensions for the limiting cases $2t/D\to 0$, 1 as shown in Fig. 1(d)–(f).

2.1. Analysis of the body force method

In this paper the stress concentration factors obtained by the body force method will be mainly used. The detail of analytical procedure may be found in [5–9]. Here, fundamental ideas will be explained by taking an example of anti-plane shear.

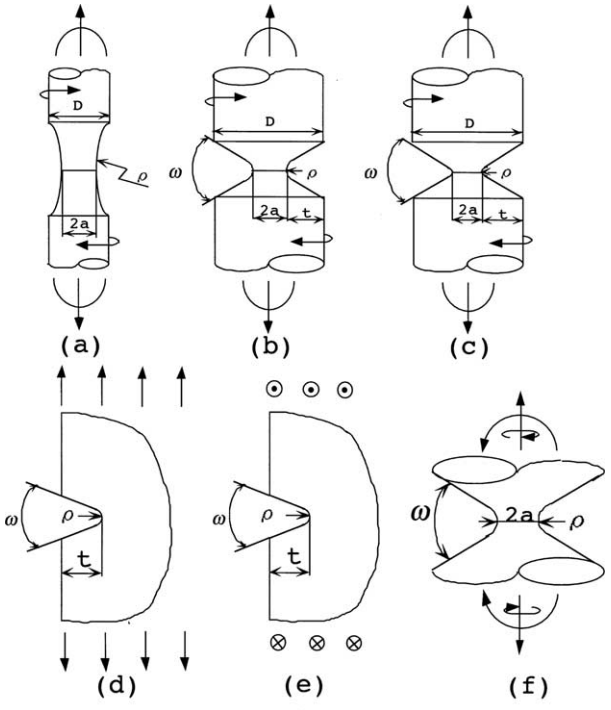

Fig. 1. Round specimens with circular-arc and V-shaped notch. (a) extremely blunt notch. (b) ordinary notch. (c) extremely sharp notch. (d) limiting case of tension and bending for $2t/D\to 0$. (e) limiting case of torsion for $2t/D\to 0$. (f) limiting case of tension, bending and torsion for $2t/D\to 1$.

Consider a semi-infinite plate having a V-shaped notch, which is composed of circular and straight parts as shown in Fig. 2.

The solution is based on superposing the stress fields due to a point force in a semi-infinite plate. To satisfy the boundary conditions, the body forces are distributed on the fictitious boundary. However, since it is difficult to determine the body force densities ρ_z in closed forms, the fictitious boundaries are divided, and the problem is solved numerically. Here, the boundary of the base of the notch (arc $\frown AB$) is divided into M_1 interval, and the boundary of the flank of the notch (line $\overline{BC}$) is divided into M_2 interval (see Fig. 2), then, constant distributions of the body force densities are assumed at each interval. Along the boundary for circular part, however, special definition of the body force densities is applied to solve the problem accurately [5,6,9].

2.2. Shallow notch

First, for the limiting case when $\lambda=2t/D\to 0$ in Fig. 1, the effect of notch opening angle will be considered for the whole range of t/ρ, that is, $t/\rho=0$–∞. Consider a semi-infinite plate having a V-shaped notch under anti-plane

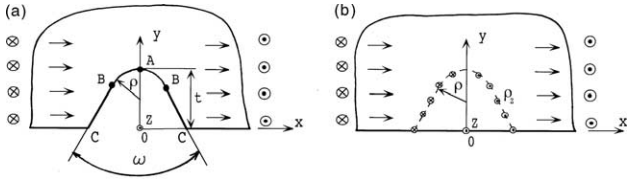

Fig. 2. (a) Anti-plane shear of a semi-infinite body with V-shaped notch (b) A fictitious boundary for V-shaped notch imagined in a semi-infinite plate, where body forces are applied.

Table 1
K_{ts}/K_{tE} for various [$K_{ts}=K_t|_{2t/D\to 0}$, $K_{ts}=1+\sqrt{t/\rho}$]

t/ρ	$\sqrt{t/\rho}$	$\omega=0°$	$\omega=40°$	$\omega=60°$	$\omega=70°$	$\omega=80°$	$\omega=90°$
0.05	0.224	0.986	0.986	0.986	0.986	0.986	0.986
0.0625	0.25	0.986	0.986	0.986	0.986	0.986	0.986
0.10	0.316	0.984	0.984	0.984	0.984	0.984	0.984
0.20	0.447	0.983	0.983	0.983	0.983	0.983	0.983
0.25	0.5	0.984	0.984	0.984	0.984	0.984	0.984
0.30	0.548	0.984	0.984	0.984	0.984	0.984	0.984
0.40	0.632	0.987	0.987	0.987	0.987	0.987	0.987
0.50	0.707	0.988	0.988	0.988	0.988	0.988	0.988
0.60	0.775	0.990	0.990	0.990	0.990	0.990	0.990
0.70	0.837	0.993	0.993	0.993	0.993	0.993	0.993
0.80	0.894	0.996	0.996	0.996	0.996	0.996	0.996
0.90	0.949	0.997	0.997	0.997	0.997	0.997	0.997
1.0	1.0	1.000	1.000	0.999	0.999	0.997	0.994
1.111	1.054	–	–	1.002	–	–	–
1.25	1.118	–	–	1.004	–	–	–
1.428	1.195	–	–	1.007	–	–	–
1.666	1.291	–	–	1.011	–	–	–
2	1.414	1.022	1.019	1.014	1.011	1.005	0.995
4	2	1.055	1.043	1.028	1.018	1.004	0.985
8	2.828	1.095	1.064	1.034	1.014	1.990	0.960
16	4	1.138	1.078	1.029	0.998	0.961	0.919
36	6	1.186	1.082	1.008	0.962	0.912	0.857
64	8	1.214	1.077	0.983	0.928	0.870	0.806
100	10	1.236	1.068	0.964	0.899	0.834	0.764
225	15	1.269	1.044	0.919	0.840	0.768	0.688
400	20	1.286	1.022	0.905	0.795	0.719	0.619
900	30	–	–	0.821	–	–	–
1600	40	–	–	0.780	–	–	–
2500	50	–	–	0.753	–	–	–
∞				0.705			

shear (see Fig. 1(e)). This corresponds to a limiting solution $K_{ts}=K_t|_{2t/D\to 0}$ in Fig. 1(a)–(c) under torsion. The analysis of the body force method indicated that the solution K_{ts} is useful for evaluating K_t if the notch is shallow or sharp [1,2,8]. Table 1 shows the results of K_{ts} for $t/\rho=0$–∞, and Table 2 explains how to obtain the results of Table 1. Tables 2 indicates the extrapolated values of K_{ts} with the values at the division number M_1 and M_2 when the notch opening angle $\omega=60$, 90° and $t/\rho=64$, 1600. Here, as an example $K_t(\to\infty(68-64))$ in Table 2 can be given from the following equation because the error due to the finite division is nearly proportional to the inverse of the division number [5,6,9].

$$K_t(\infty(68-64))=\frac{68\times K_t(68)-64\times K_t(64)}{68-64}$$

Table 2
Convergence of K_{ts}

$t/\rho=64$			$t/\rho=1600$		
M_1	M_2	$\omega=90°$	M_1	M_2	$\omega=60°$
64	400	7.2520	30	1500	31.8686
68	432	7.2522	31	1550	31.8728
72	464	7.2524	32	1600	31.8764
76	496	7.2525	33	1650	31.8797
$\to\infty$ (68−64)		7.2556	$\to\infty$ (31−30)		31.9976
$\to\infty$ (72−68)		7.2552	$\to\infty$ (32−31)		31.9905
$\to\infty$ (76−72)		7.2547	$\to\infty$ (33−32)		31.9803
K_{tE}		9	K_{tE}		41

From Table 2, it is seen that the present results in Table 1 have four-digit accuracy because two extrapolated values coincide with each other to the fourth digit.

Table 1 indicates that the effect of notch opening angle is negligibly small $t/\rho\le 1.0$. However, the effect is significant if $t/\rho>1.0$. In other words, K_{ts} increases with decreasing the notch opening angle ω if $t/\rho>1.0$. The effect of ω is significant, especially when $t/\rho\to\infty$. The results of Table 1 is plotted in Fig. 3(a) in comparison with the results in Fig. 3(b) under tension, which is corresponding to the limiting solution $K_{ts}=K_t|_{2t/D\to 0}$ in Fig. 1(a)–(c) under tension and bending. In Fig. 3, it should be noted that the effect of notch opening angle under torsion is much larger than the one under tension and bending. As an example, when $t/\rho=400$, the result of $\omega=0°$ is about twice larger than the results of $\omega=90°$ under torsion. However, the result of $\omega=0°$ is larger only by 17% than the results of $\omega=90°$ under tension when $t/\rho=400$.

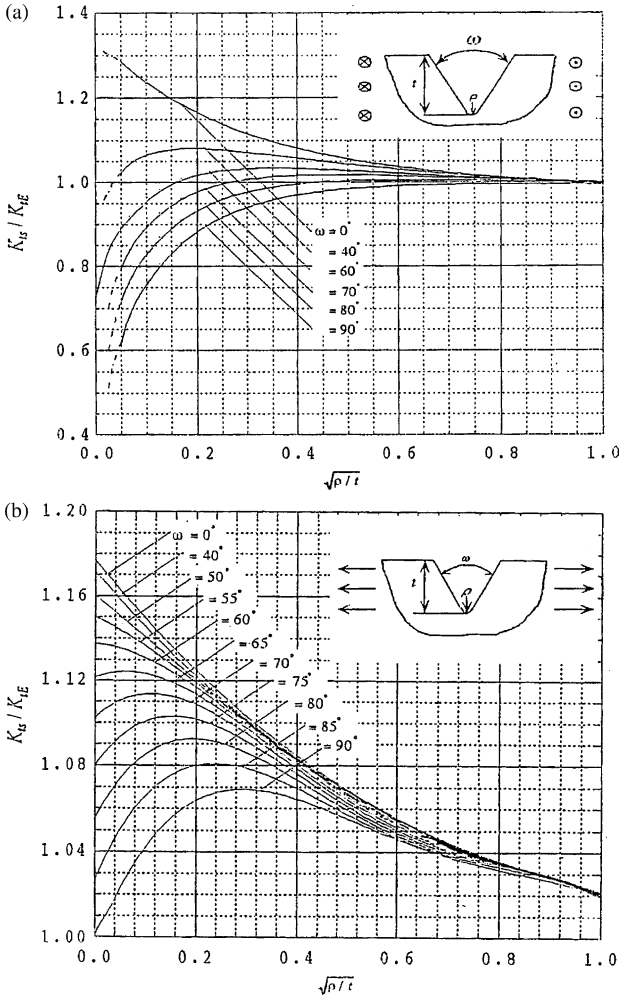

Fig. 3. K_{ts}/K_{tE} vs. $\sqrt{\rho/t}$ for (a) torsion and (b) tension.

Table 3
Convergence of K_t when $\omega=60°$ under torsion

M_1	M_2	$a/\rho=1.0$		
		$2t/D=0.7$	$2t/D=0.8$	$2t/D=0.9$
10	30	1.14779	1.14795	1.14798
15	45	1.14786	1.14802	1.14806
20	60	1.14789	1.14804	1.14809
$\to\infty$ (15−10)		1.14801	1.14817	1.14822
$\to\infty$ (20−15)		1.14796	1.14812	1.14817
$K_{t\mathrm{H}}$		1.142	1.142	1.142

2.3. Deep notch

Next, a deep V-shaped notch in Fig. 1(f) under torsion will be considered as a limiting solution $K_{t\mathrm{d}}=K_t|_{2t/D\to 1}$ in Fig. 1(a)–(c). The previous study indicated that the solution $K_{t\mathrm{d}}$ is useful for evaluating K_t if the notch is deep or blunt [1,2,9,10]. Here, $K_{t\mathrm{d}}$ is obtained in the following way. In Tables 3, several example results of the body force method are indicated [9]. Here, K_t values are extrapolated from the results at the division number M_1 and M_2 when the notch opening angle $\omega=60°$ and $a/\rho=1.0$. From Table 3, it is seen that the results have four-digit accuracy. Table 4 shows the ratio $K_t/K_{t\mathrm{H}}$ when $2t/D=0.7$, 0.8, 0.9, where K_t is calculated as shown in Table 3, and $K_{t\mathrm{H}}$ is a SCF of a deep hyperboloidal notch [3]. With increasing notch depth, $K_t/K_{t\mathrm{H}}$ approaches limiting values, namely, $K_t/K_{t\mathrm{H}}\to$ (1.000–1.052) when $\omega=60°$. The ratio $K_t/K_{t\mathrm{H}}$ does not approach unity because of the difference of the notch shape; 60° V notch and hyperboid. In Table 5, the limiting values of $K_{t\mathrm{d}}/K_{t\mathrm{H}}$ are obtained using the convergence of $K_t/K_{t\mathrm{H}}$ when $2t/D\to 1.0$ when $\omega=0$–90°.

Table 4
$K_t/K_{t\mathrm{H}}$ for when $2t/D\to 1.0$ and $\omega=60°$ under torsion

	a/ρ	ρ/a	$2t/D=0.7$	$2t/D=0.8$	$2t/D=0.9$	$2t/D\to 1.0$
0.000	0.000	∞	1.000	1.000	1.000	1.000
0.100	0.100	10.00	1.000	1.000	1.001	1.001
0.200	0.200	5.000	1.000	1.000	1.000	1.000
0.300	0.300	3.333	1.001	1.001	1.001	1.001
0.400	0.400	2.500	1.001	1.001	1.001	1.001
0.500	0.500	2.000	1.002	1.002	1.002	1.002
0.600	0.600	1.667	1.003	1.003	1.003	1.003
0.700	0.700	1.429	1.004	1.004	1.004	1.004
0.800	0.800	1.250	1.004	1.004	1.004	1.004
0.900	0.900	1.111	1.005	1.005	1.004	1.004
1.000	1.000	1.000	1.005	1.005	1.005	1.005
1.000	1.000	1.000	1.005	1.005	1.005	1.005
1.100	1.111	0.900	1.007	1.007	1.007	1.007
1.200	1.250	0.800	1.007	1.007	1.008	1.008
1.300	1.429	0.700	1.009	1.009	1.009	1.009
1.400	1.667	0.600	1.011	1.011	1.011	1.011
1.500	2.000	0.500	1.014	1.014	1.014	1.014
1.600	2.500	0.400	1.017	1.017	1.018	1.018
1.700	3.333	0.300	1.022	1.023	1.024	1.024
1.800	5.000	0.200	1.030	1.031		1.031
1.900	10.00	0.100	1.042			1.042
2.000	∞	0.000				1.052

Table 5
$K_t/K_{t\mathrm{H}}$ for various ω when $2t/D\to 1.0$ under torsion

x	a/ρ	ρ/a	$\omega=0°$	$\omega=60°$	$\omega=90°$
0.000	0.000	∞	1.000	1.000	1.000
0.100	0.100	10.00	1.001	1.001	1.001
0.200	0.200	5.000	1.000	1.000	1.000
0.300	0.300	3.333	1.001	1.001	1.001
0.400	0.400	2.500	1.001	1.001	1.001
0.500	0.500	2.000	1.002	1.002	1.002
0.600	0.600	1.667	1.003	1.003	1.003
0.700	0.700	1.429	1.004	1.004	1.004
0.800	0.800	1.250	1.004	1.004	1.004
0.900	0.900	1.111	1.005	1.004	1.005
1.000	1.000	1.000	1.005	1.005	1.005
1.000	1.000	1.000	1.005	1.005	1.005
1.100	1.111	0.900	1.007	1.007	1.006
1.200	1.250	0.800	1.008	1.008	1.007
1.300	1.429	0.700	1.009	1.009	1.008
1.400	1.667	0.600	1.011	1.011	1.010
1.500	2.000	0.500	1.014	1.014	1.011
1.600	2.500	0.400	1.018	1.018	1.014
1.700	3.333	0.300	1.027	1.024	1.017
1.800	5.000	0.200	1.040	1.031	1.017
1.900	10.00	0.100	1.081	1.042	1.018
2.000	∞	0.000	1.090	1.052	1.019

The $K_{t\mathrm{d}}=K_t|_{2t/D\to 1}$ can be expressed as a function of the parameter x for the whole range. The results of Table 5 are plotted in Fig. 4 in comparison with the cases under tension and bending.

The stress concentration factor (SCF) usually decreases with increasing the notch opening angle. However, in Fig. 4(b), it is seen that the SCF under tension sometimes increases with increasing the notch opening angle. The effect of notch opening angle is comparatively larger for deep notches under bending. In torsion, as $\rho\to 0$, the difference between the results of $\omega=0$ and 90° becomes larger, about 7%, which is corresponding to 5% for tension. However, generally speaking, for deep notches under torsion and tension, the effect of ω is not very large.

3. Stress concentration factors of shallow and sharp notches.

Generally, it is believed that if t/ρ is constant the effect of notch opening angle is not very large in the range of $\omega=0$–90°. In the previous discussion, however, it is found that for a shallow notch under torsion the effect of notch opening angle is quite large. It should be noted that the effect of notch opening angle is significant in fatigue test specimen for the shallow notch under torsion and for the deep notch under bending. In this study, the angle is fixed as $\omega=60°$, then the stress concentration formula useful for any dimensions of notch will be considered. The formulas useful for $\omega=0$–90° will be investigated in the next papers. First, by applying least squares method, two limiting solutions are obtained as K_{ts} and $K_{t\mathrm{d}}$ useful for all range of t/ρ and a/ρ, respectively (see Fig. 1(d)–(f)).

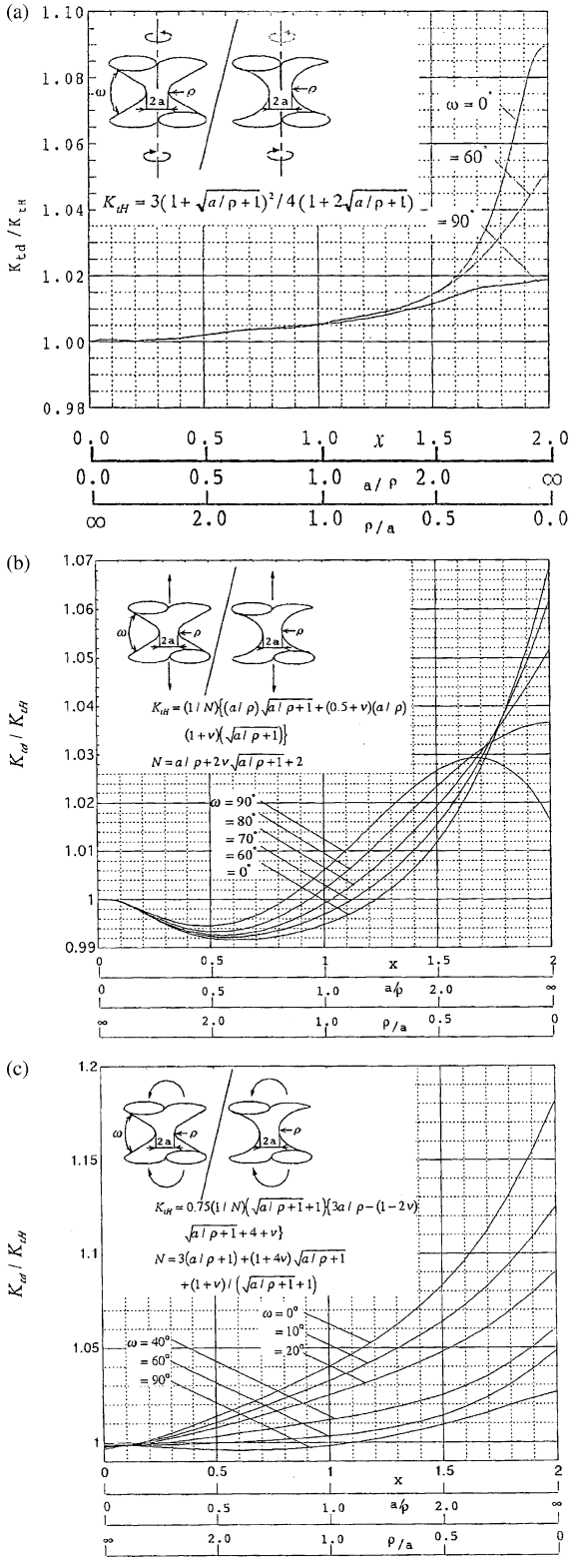

Fig. 4. K_{td}/K_{tH} vs. a/ρ or ρ/a under (a) torsion (b) tension (c) bending.

Consider the stress concentration factor K_t of a sharp notch as shown in Fig. 1(c). In this case, the SCF is mainly controlled by the SCF of a notch in a semi-infinite plate K_{ts} having the same shape ratio t/ρ. The ratio K_t/K_{ts} is shown in Fig. 5 for the wide range of the notch radius ($0 < \rho/a \leq 10$) in

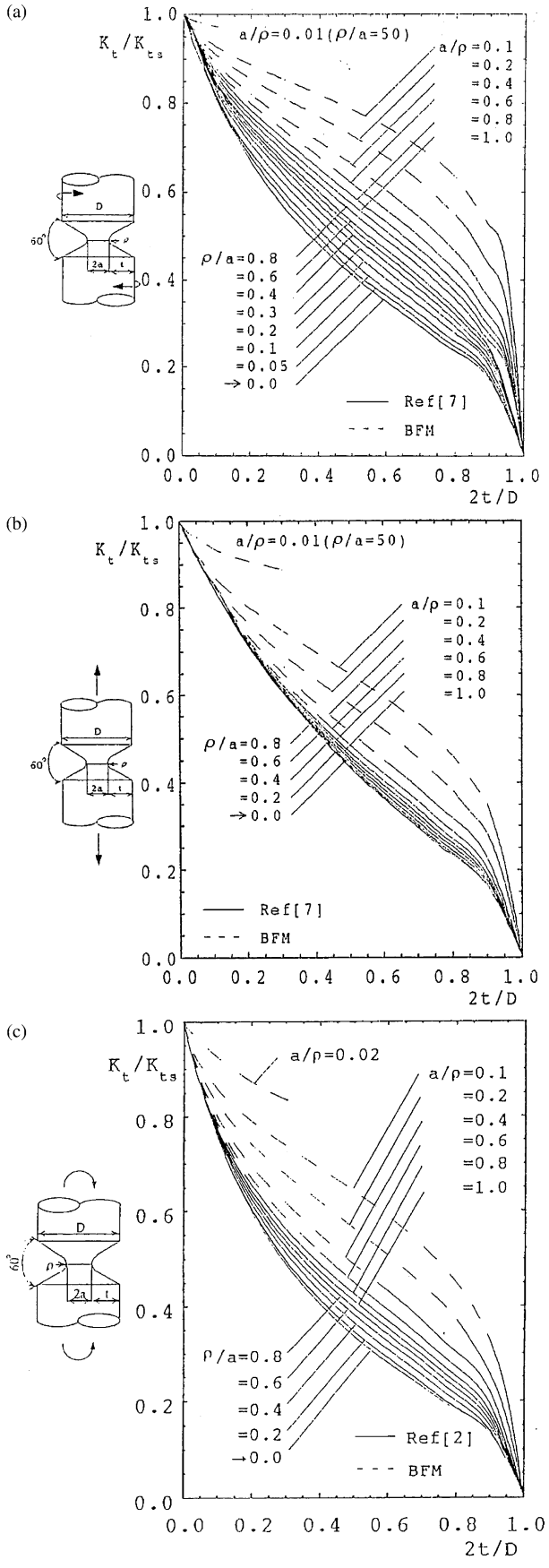

Fig. 5. K_t/K_{ts} vs. $2t/D$ for (a) torsion (b) tension (c) bending.

comparison with the case under tension and bending. In these figures, the solid lines are given form the formulas proposed in the previous papers [11,12], and the dashed lines are given form newly applying the body force method. The lines for $\rho/a \to 0$ is given from the results for generalized stress intensity factors of sharp notches [13]. From the comparison of the results, it is found that the value of K_t/K_{ts} under torsion is distributed in the wider area. In other words, the K_{ts} solution can be a better approximation for K_t in tension and bending because K_t/K_{ts} is distributed in the narrower area. However, from Fig. 5(a), we can see that:

(1) Even for sharp notches under torsion, for example, in the range of $\rho/a \leq 0.05$, the value of K_t/K_{ts} is not determined by $2t/D$ alone, different from the case of tension and bending. However, since the values of K_t/K_{ts} for $\rho/a = 0.05$ and $\rho/a \to 0$ are very close, the value of K_t/K_{ts} for $\rho/a \leq 0.05$ may be estimated well from K_{ts}.
(2) For shallow notches, $2t/D \leq 0.02$, the value of K_t/K_{ts} is almost controlled by the notch depth $2t/D$ except for the case of $a/\rho \leq 0.01$. For example, when $2t/D = 0.02$, the K_t/K_{ts} value is in the small range of $K_t/K_{ts} = 0.956$–0.989.
(3) When the notch is blunt and shallow, the stress concentration factor will be considered (see the next section). Then, the stress concentration factor is found to be in the range $K_t = (1.000$–$1.002)$ if $2t/D \leq 0.02$ and $a/\rho \leq 0.01$.

4. Stress concentration factors of blunt and deep notches

Here, the SCF is considered for blunt and deep notches. In this case, the SCF of a deep hyperboloidal notch $K_{t\mathrm{H}}$ [1] can be used as a good approximate formula, that is, $K_t/K_{t\mathrm{H}} \cong 1$ [1,2,9]. As shown in Section 2.2, the deep notch ($2t/D \geq 0.7$) can be estimated more accurately as an infinitely deep notch as shown in Fig. 6.

Fig. 7 shows the ratio $K_t/K_{t\mathrm{d}}$ under torsion in comparison with the case under bending and tension. As shown in Fig. 7, the value of $K_t/K_{t\mathrm{d}}$ is in a narrow range in torsion. In other words, $K_{t\mathrm{d}}$ in torsion can be a better approximation than $K_{t\mathrm{d}}$ in tension and bending.

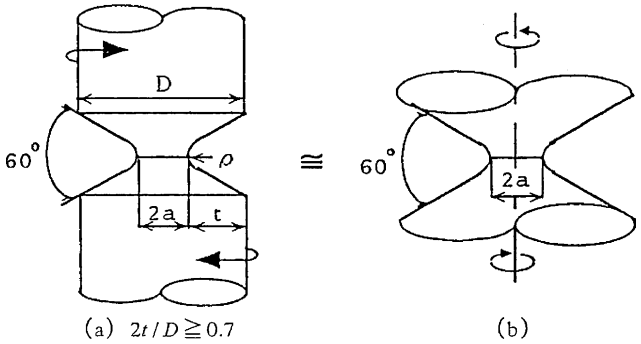

Fig. 6. K_t and $K_{t\mathrm{d}}$ with V-shaped notches.

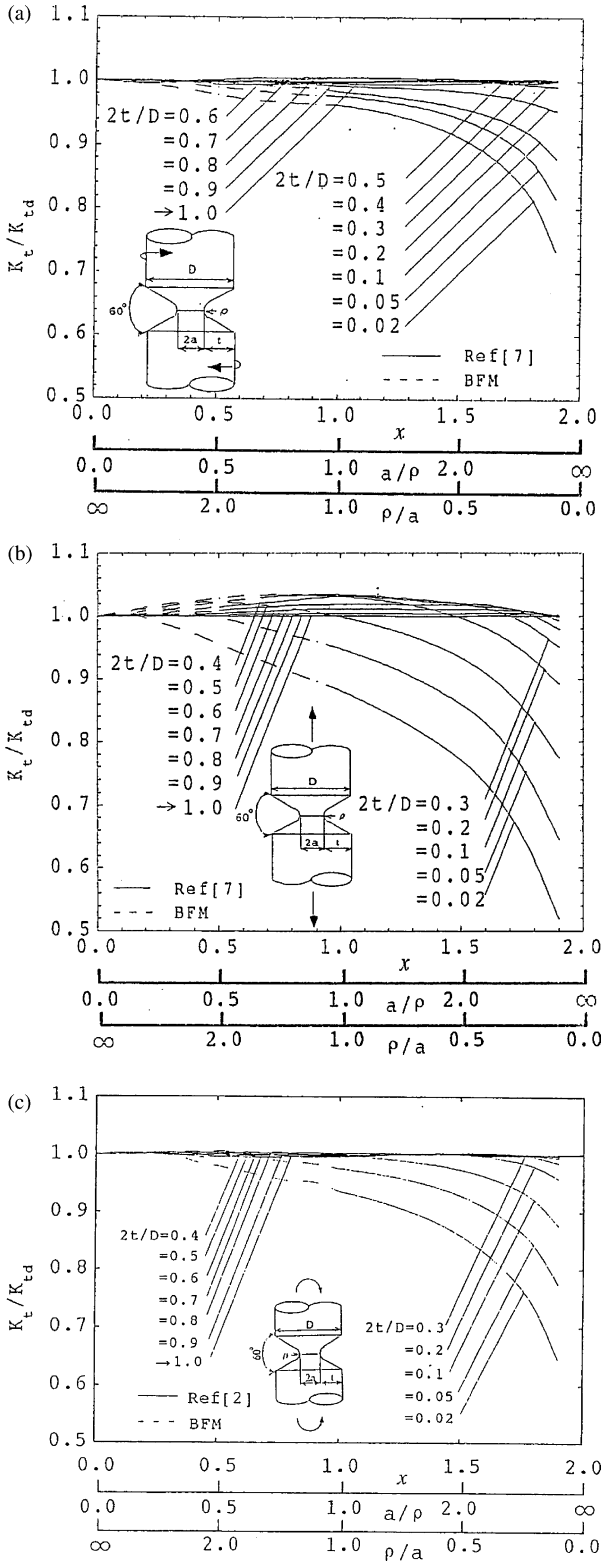

Fig. 7. $K_t/K_{t\mathrm{d}}$ vs. a/ρ or ρ/a for (a) torsion (b) tension (c) bending.

From Fig. 7(a), it is seen that the $K_{t\mathrm{d}}$ approximation is useful in the following range.

(1) $2t/D \geq 0.4$, $20 \leq a/\rho \leq \infty$; $0.985 \leq K_t/K_{t\mathrm{d}} \leq 1.001$

(2) $0.2 \le 2t/D \le 1.0$, $0 \le a/\rho \le 20$; $0.984 \le K_t/K_{td} \le 1.006$
(3) $0.02 \le 2t/D \le 0.2$, $0 \le a/\rho \le 2.0$; $0.912 \le K_t/K_{td} \le 1.000$

In torsion, the K_{ts} solution cannot be a good approximation for K_t; however, the K_{td} solution can be a better approximation for K_t. Considering these facts, we can make a good approximation formula for torsion problem.

5. Stress concentration factors of other notches under torsion

Here, the stress concentration factor K_t is considered for the remaining region under torsion, that is, $0.05 \le \rho/a \le 0.5$, $0.02 \le 2t/D \le 0.2$. In this region, as shown in Fig. 5 the values of K_t/K_{ts} is mainly controlled by $2t/D$, and then they are in a narrow range. Fig. 8 shows $K_t/K_{ts}/[K_t/K_{ts}]_{\rho/a=0.2}$. From Fig. 8, it is seen that $K_t/K_{ts}/[K_t/K_{ts}]_{\rho/a=0.2} = (0.96\text{–}1.05)$ if $0.05 \le \rho/a \le 0.5$ and $0 \le 2t/D \le 0.2$.

6. A set of SCF formulas useful for any dimensions of notch under torsion

From the above discussion, any shape of the notch has been classified into one of the groups shown in Fig. 9. Then, the least squares method is applied to each region shown in Fig. 9.

Finally, a set of accurate formulas for the whole range of notch shapes are obtained. The results are as follows.

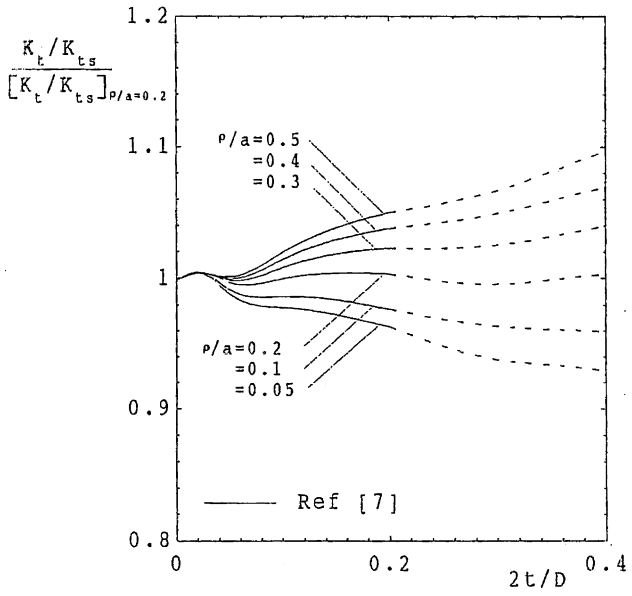

Fig. 8. $(K_t/K_{ts})/([K_t/K_{ts}]_{\rho/a=0.2})$ vs. $2t/D$ under torsion.

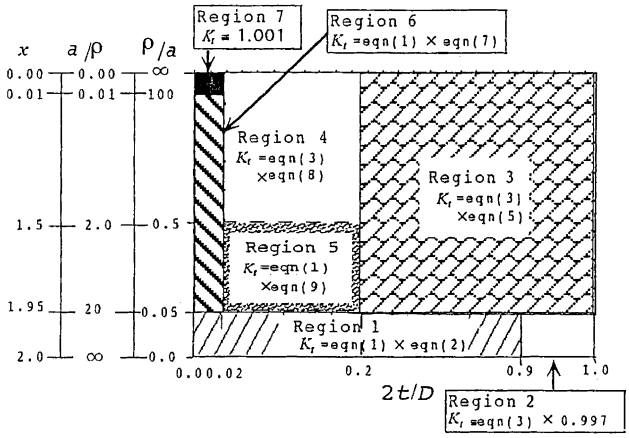

Fig. 9. Classification of notch shape under torsion. Region 1, sharp and shallow notch; Region 2, sharp and deep notch; Region 3, deep notch; Region 4, blunt notch; Region 5, ordinary notch; Region 6, shallow notch; Region 7, blunt and shallow notch.

SCF OF A NOTCH IN A SEMI-INFINITE PLATE K_{ts} (If ρ, t are fixed, and as d, $D \to \infty$ in Fig. 1, $K_t \to K_{ts}$).

The limiting SCF of shallow notch $K_t \to K_{ts}$ in Fig. 1 when a, $D \to \infty$. The K_{ts} formula can be expressed in Eq. (1).

(1) $0 \le \xi \le 1.0$

$$K_{ts}/K_{tE} = 1.000 - 0.089464\xi + 0.13872\xi^2 - 0.050088\xi^3 \quad (1a)$$

(2) $0 \le \eta \le 0.05$

$$K_{ts}/K_{tE} = 0.70516 - 0.77340\eta + 200.235\eta^2 - 2106.840\eta^3 \quad (1b)$$

(3) $0.05 < \eta < 1.0$

$$K_{ts}/K_{tE} = 0.81595 + 2.0675\eta - 7.2824\eta^2 + 12.045\eta^3 - 9.6241\eta^4 + 2.9783\eta^5 \quad (1c)$$

$$\xi = \sqrt{t/\rho}, \qquad \eta = \sqrt{\rho/t}, \qquad K_{tE} = 1 + \sqrt{t/\rho} \quad (1d)$$

Fig. 10 indicates the value of K_{ts}/K_{tE} using Eq. (1).

SCF OF A SHARP OR SHALLOW NOTCH K_t (Region 1 in Fig. 9: $\rho/a \le 0.05$ and $2t/D \le 0.4$)

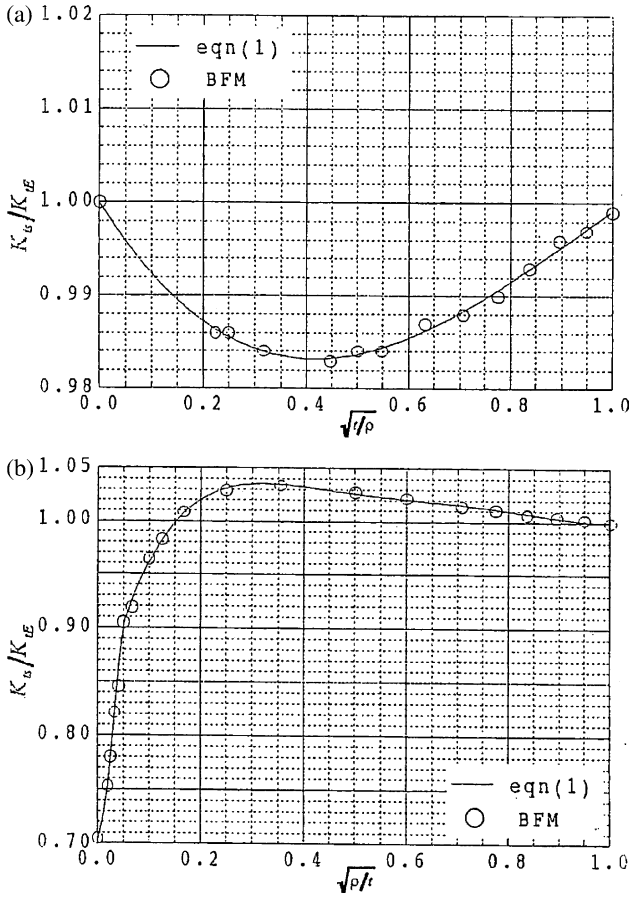

Fig. 10. K_{ts}/K_{tE} vs.$\sqrt{t/\rho}$ and $\sqrt{\rho/t}$ under torsion.

$$K_t/K_{ts} = 1.0002 + 0.065000(\rho/a) - 0.46000(\rho/a)^2 + \{-2.3204 + 41.027(\rho/a) - 272.908(\rho/a)^2\}\lambda + \{4.9383 - 1051.719(\rho/a) + 7281.060(\rho/a)^2\}\lambda^2 + \{-14.354 + 9977.270(\rho/a) - 69,683.800(\rho/a)^2\}\lambda^3 + \{57.094 - 47,562.010(\rho/a) + 334,477.80(\rho/a)^2\}\lambda^4 + \{-189.604 + 128,887.31(\rho/a) - 911,641.40(\rho/a)^2\}\lambda^5 + \{398.124 - 207,815.03(\rho/a) + 1476,793.4(\rho/a)^2\}\lambda^6 + \{-487.188 + 197,560.60(\rho/a) - 1409,226.4(\rho/a)^2\}\lambda^7 + \{317.414 - 102,277.81(\rho/a) + 731,834.20(\rho/a)^2\}\lambda^8 + \{-85.103 + 22,240.230(\rho/a) - 159,561.00(\rho/a)^2\}\lambda^9 \quad (2a)$$

$$\lambda = 2t/D \quad (2b)$$

The value of Eq. (2) is shown in Fig. 11.

SCF OF A DEEP NOTCH K_t (If a, ρ are fixed, and $t\rightarrow\infty$, $K_t\rightarrow K_{td}$)

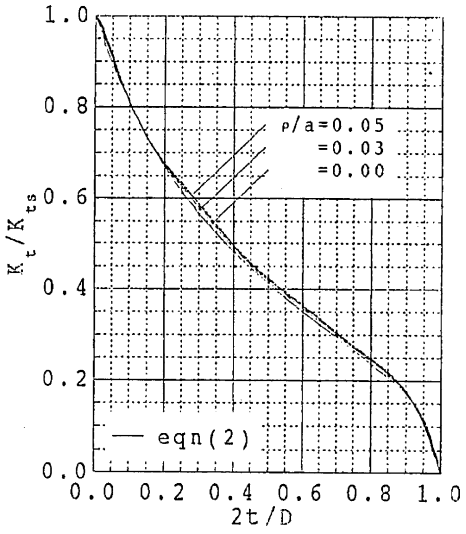

Fig. 11. K_t/K_{ts} vs. $2t/D$ under torsion.

$$K_{td}/K_{tH} = 1.0004 - 0.0054166x + 0.031712x^2 - 0.034608x^3 + 0.013315x^4, \quad (3)$$

$$K_{tH} = 3(1+\sqrt{a/\rho+1})^2/4(1+2\sqrt{a/\rho+1})$$

Fig. 12 indicates the value K_{td}/K_{tH}.

SCF of SHARP AND DEEP NOTCH (Region 2 in Fig. 9: $\rho/a \leq 0.05$ and $2t/D \geq 0.9$)

$$K_t/K_{td} \cong 0.997 \quad (4)$$

SCF OF DEEP NOTCH (Region 3 in Fig. 9: $\lambda = 2t/D \geq 0.2$ and $a/\rho \geq 20$ $(0 \leq x \leq 1.95)$)

$$K_t/K_{td} = (1.2732 - 5.2256\lambda + 41.037\lambda^2 - 173.861\lambda^3 + 436.177\lambda^4 - 666.588\lambda^5 + 609.405\lambda^6 - 306.425\lambda^7 + 65.207\lambda^8) + (-3.9187 + 74.205\lambda - 573.456\lambda^2 + 2380.186\lambda^3 - 5824.853\lambda^4 + 8649.916\lambda^5 - 7658.407\lambda^6 + 3718.693\lambda^7 - 762.3645\lambda^8)x + (11.100 - 210.828\lambda + 1633.779\lambda^2 - 6808.307\lambda^3 + 16,762.089\lambda^4 - 25,112.854\lambda^5 + 22,504.266\lambda^6 - 11,095.586\lambda^7 + 2316.340\lambda^8)x^2 + (-10.339 + 196.614\lambda - 1527.889\lambda^2 + 6393.566\lambda^3 - 15,824.185\lambda^4 + 23,855.548\lambda^5 - 21,525.758\lambda^6 + 10,690.755\lambda^7 - 2248.312\lambda^8)x^3 + (2.9974$$

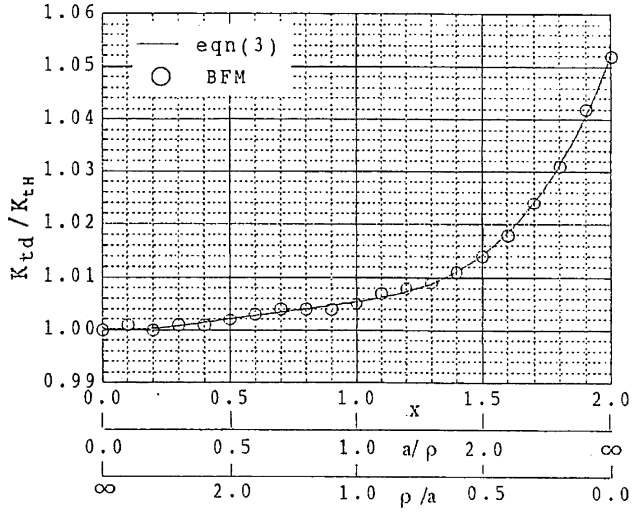

Fig. 12. K_{td}/K_{tH} vs. a/ρ or ρ/a under torsion.

$$-57.230\lambda+445.993\lambda^2-1871.177\lambda^3+4643.677\lambda^4$$
$$-7020.090\lambda^5+6351.932\lambda^6-3462.667\lambda^7$$
$$+666.564\lambda^8)x^4 \tag{5}$$

SCF OF BLUNT AND SCHALLOW NOTCH (Region 7 in Fig. 9: $a/\rho \le 0.01$, $2t/D \le 0.02$)

$$K_t \cong 1.001 \tag{6}$$

SCF OF SCHALLOW NOTCH (Region 6 in Fig. 9: $0.01 \le a/\rho \le 20$ ($0.01 \le x \le 1.95$) and $2t/D \le 0.02$)

$$K_t/K_{ts} = 1.000-(1.0552+1.8464x+1.9736x^2$$
$$-8.2590x^3+6.1096x^4-1.3570x^5) \tag{7}$$

SCF OF BLUNT NOTCH (Region 4 in Fig. 9: $a/\rho \le 2.0$ ($0 \le x \le 1.5$) and $0.02 \le 2t/D \le 0.2$)

$$K_t/K_{td} = (1.0016-0.070219\lambda+0.77019\lambda^2-2.3148\lambda^3)$$
$$+(-0.040827+2.2659\lambda-26.359\lambda^2+80.467\lambda^3)x$$
$$+(-0.14433-1.7471\lambda+46.228\lambda^2-169.806\lambda^3)x^2$$
$$+\left(0.22594+0.033869\lambda-36.720\lambda^2+153.290\lambda^3\right)x^3$$
$$+\left(-0.098744+0.48288\lambda+8.4604\lambda^2-41.490\lambda^3\right)x^4 \tag{8}$$

OTHER NOTCH (Region 5 in Fig. 9: $0.05 \le \rho/a \le 0.5$ ($1.5 \le x \le 1.95$) and $0.02 \le \lambda = 2t/D \le 0.2$)

$$K_t/K_{ts} = \{(1.0005+0.0051162(\rho/a)-0.11705(\rho/a)^2$$
$$+0.60862(\rho/a)^3-1.2770(\rho/a)^4+0.95132(\rho/a)^5)$$
$$+(0.046366-2.8738(\rho/a)+41.066(\rho/a)^2$$
$$-206.252(\rho/a)^3+423.882(\rho/a)^4-309.132(\rho/a)^5)\lambda$$
$$+(-5.7618+64.791(\rho/a)-516.761(\rho/a)^2$$
$$+2384.219(\rho/a)^3-4832.939(\rho/a)^4+3527.542(\rho/a)^5)\lambda^2$$
$$+(21.719-235.937(\rho/a)+1785.138(\rho/a)^2$$
$$-7871.300(\rho/a)^3+15{,}633.377(\rho/a)^4$$
$$-11{,}306.862(\rho/a)^5)\lambda^3\}([K_t/K_{ts}]_{\rho/a=0.2}) \tag{9a}$$

$$[K_t/K_{ts}]_{\rho/a=0.2} = 1.0019-0.96607\lambda-23.944\lambda^2$$
$$+254.767\lambda^3-1220.738\lambda^4+3272.556\lambda^5$$
$$-5196.867\lambda^6+4851.327\lambda^7$$
$$-2457.932\lambda^8+520.795\lambda^9 \tag{9b}$$

A set of formulas given by Eqs. (1)–(9) gives accurate stress concentration factors, K_t for the whole range of notches.

7. Simple formulas for any dimensions of notch

By fitting smooth curves to Eqs. (1)–(9), a convenient formula can be proposed. Here, to improve the accuracy another approximate formulas are used. Also, the body force method is applied again to confirm accurate K_t values when some differences are observed between the equations. First, a modified Neuber formula $K_{tN}^{m=2.6}$ for notch is expressed by [10,11]

$$K_{tN}^{m=2.6} = \{(K_{ts}-1)(K_{td}-1)/((K_{ts}-1)^{2.6} + (K_{td}-1)^{2.6})^{1/2.6}\}+1 \tag{10}$$

The error of Eq. (10) is estimated about within 15%. Then, the least squares method is applied to K_t/K_{tN}, where K_t is the value of Eqs. (1)–(9). Fig. 13 and Eqs. (11a)–(11e) express correction factors of K_t/K_{tN}. The formulas give SCFs within 1% error in most cases for any dimensions of notch.

(1) $0 < x \le 1.95$

$$K_t/K_{tN}^{m=2.6} = 0.99999-0.0026822x+0.0053295x^2-0.0016953x^3$$
$$+(0.0026579-0.32756x+0.031522x^2-0.081859x^3)\lambda$$
$$+(-0.0076275+6.1229x-4.8157x^2+2.3235x^3)\lambda^2$$
$$+(-0.23987-30.899x+30.141x^2-12.484x^3)\lambda^3$$
$$+(1.0501+63.622x-66.952x^2+26.072x^3)\lambda^4$$
$$+(-1.4274-57.780x+63.046x^2-23.742x^3)\lambda^5$$
$$+(0.62212+19.268x-21.460x^2+7.9153x^3)\lambda^6 \tag{11a}$$

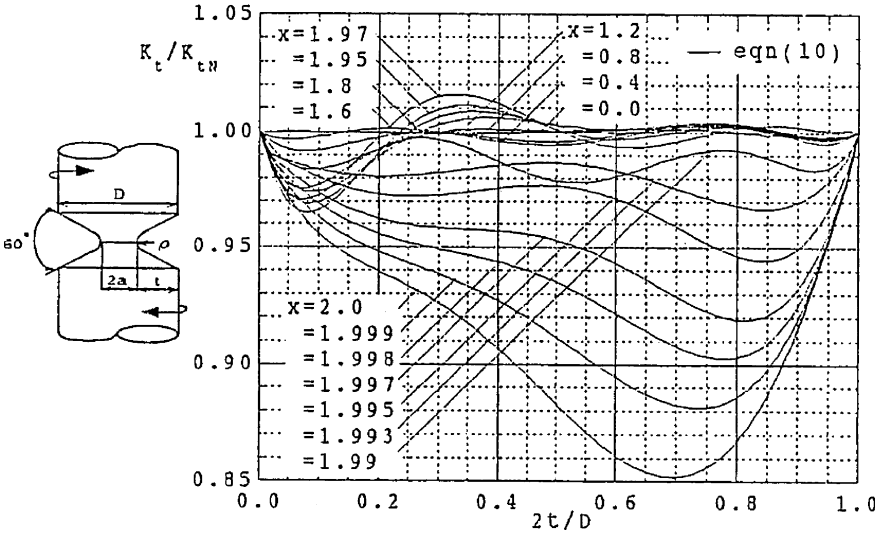

Fig. 13. K_t/K_{tN} vs. $2t/D$ under torsion.

(2) $1.95 < x \le 1.99$

$$\begin{aligned} K_t/K_{tN}^{m=2.6} &= 1.0025 - 0.0093115A - 0.0058186A^2 + 0.025526A^3 \\ &+ (-1.1232 + 0.77408A + 0.76457A^2 - 1.5432A^3)\lambda \\ &+ (10.849 - 5.3371A - 6.5696A^2 + 12.729A^3)\lambda^2 \\ &+ (-38.451 + 23.186A + 9.7978A^2 - 98.794A^3)\lambda^3 \\ &+ (63.849 - 53.490A + 9.3650A^2 + 285.633A^3)\lambda^4 \\ &+ (-50.412 + 56.678A - 27.335A^2 - 328.903A^3)\lambda^5 \\ &+ (15.286 - 21.788A + 13.972A^2 + 130.778A^3)\lambda^6 \end{aligned} \tag{11b}$$

$$A = 10(x - 1.95) \tag{11c}$$

(3) $1.99 < x \le 2.0$

$$\begin{aligned} K_t/K_{tN}^{m=2.6} &= 0.99192 + 0.00011120B + 0.0033482B^2 + 0.0013571B^3 \\ &+ (-0.18992 + 0.41943B - 0.32590B^2 - 0.54245B^3)\lambda \\ &+ (1.5804 - 5.6709B + 1.6900B^2 + 5.3873B^3)\lambda^2 \\ &+ (-4.6494 + 21.058B - 4.1818B^2 - 19.802B^3)\lambda^3 \\ &+ (5.5040 - 28.913B + 4.0856B^2 + 27.079B^3)\lambda^4 \\ &+ (-2.2419 + 13.113B - 1.2682B^2 - 12.130B^3)\lambda^5 \end{aligned} \tag{11d}$$

$$B = 100(x - 1.99) \tag{11e}$$

In Eq. (11), $K_{tN}^{m=2.6}$ is given by Eq. (10), K_{ts} is given by Eq. (1), and K_{td} is given by Eq. (3).

Similarly, the stress concentration formula under tension and bending can be given by the following equations [1,2].

(1) For Tension ($0 \le 2t/D \le 1.0$, $0 \le x \le 2.0$)

$$\begin{aligned} K_t/K_{tN}^{m=2.8} &= (1.0001 + 0.0036x - 0.0065x^2 + 0.0021x^3) \\ &+ (0.0116 + 1.404x - 1.285x^2 + 0.1799x^3)\lambda \\ &+ (-0.1311 - 8.165x + 9.687x^2 - 2.124x)\lambda^2 \\ &+ (0.4240 + 16.94x - 22.77x^2 + 5.618x)\lambda^3 \\ &+ (-0.5156 - 15.07x + 21.71x^2 - 5.571x)\lambda^4 \\ &+ (0.2112 + 4.890x - 7.332x^2 + 1.896x)\lambda^5, \end{aligned} \tag{12a}$$

$$K_{tN}^{m=2.8} = \{(K_{ts} - 1)(K_{td} - 1)/((K_{ts} - 1)^{2.8} + (K_{td} - 1)^{2.8})^{1/2.8}\} + 1 \tag{12b}$$

where

$$\begin{aligned} K_{ts}/K_{tE} &= 1.000 - 0.127\xi + 0.2908\xi^2 - 0.1420\xi^3 \\ &\quad (\text{if } 0 \le \xi \le 1.0) \end{aligned} \tag{12c}$$

$$\begin{aligned} K_{ts}/K_{tE} &= 1.148 - 0.160\eta - 0.0345\eta^2 + 0.0693\eta^3 \\ &\quad (\text{if } 0 \le \eta \le 1.0) \end{aligned} \tag{12d}$$

$$\xi = \sqrt{t/\rho}, \qquad \eta = \sqrt{\rho/t}, \qquad K_{tE} = 1 + \sqrt{t/\rho} \tag{12e}$$

$$\begin{aligned} K_{td}/K_{tH} &= 1.0011 - 0.025485x + 0.006131x^2 \\ &\quad + 0.006131x^3 \end{aligned} \tag{12f}$$

$$\begin{aligned} K_{tH} &= (1/N)\left\{(a/\rho)\left(\sqrt{a/\rho + 1} + 1\right)(0.5 + \nu)(a/\rho)\right. \\ &\quad \left. + (1 + \nu)\left(\sqrt{a/\rho + 1} + 1\right)\right\}, \\ N &= a/\rho + 2\nu\sqrt{a/\rho + 1} + 2 \end{aligned} \tag{12g}$$

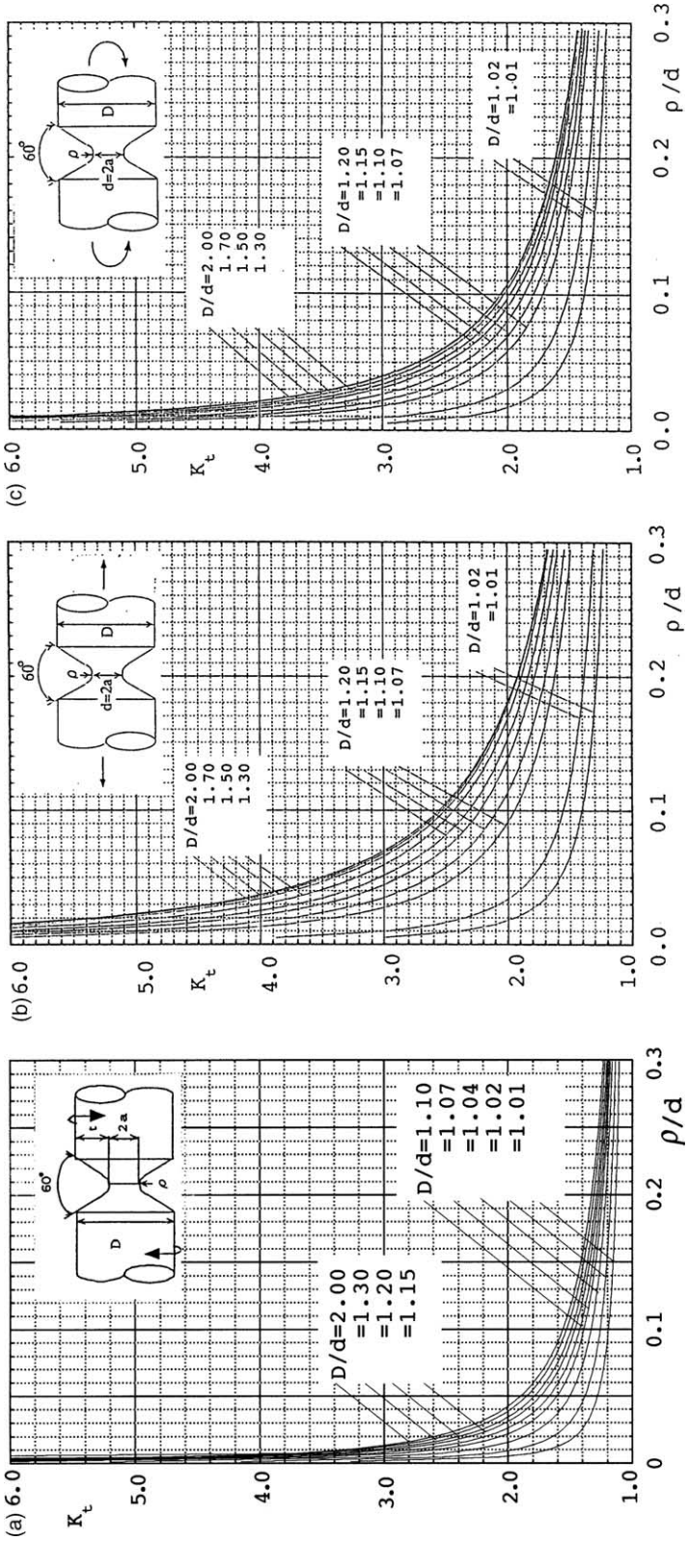

Fig. 14. K_t vs. ρ/d for (a) torsion, (b) tension, (c) bending.

(2) For Bending ($0 \le 2t/D \le 1.0$, $0 \le x \le 2.0$)

$$\begin{aligned} K_t/K_{t\mathrm{N}}^{m=2.8} &= (1.0026 - 0.0054x - 0.0023x^2 + 0.0011x^3) \\ &+ (-0.0157 + 0.3076x + 0.0246x^2 - 0.2020x^3)\lambda \\ &+ (0.1164 - 2.516x + 0.9511x^2 - 0.9811x)\lambda^2 \\ &+ (-0.2195 + 2.893x - 3.103x^2 - 1.964x)\lambda^3 \\ &+ (0.1342 - 5.328x + 3.153x^2 + 1.850x)\lambda^4 \\ &+ (-0.0159 + 1.643x - 1.021x^2 - 0.6666x)\lambda^5 \end{aligned} \tag{13a}$$

$$K_{t\mathrm{N}}^{m=2.8} = \{(K_{ts} - 1)(K_{td} - 1)/((K_{ts} - 1)^{2.8} + (K_{td} - 1)^{2.8})^{1/2.8}\} + 1 \tag{13b}$$

where

$$K_{ts}/K_{t\mathrm{E}} = 1.000 - 0.127\xi + 0.2908\xi^2 - 0.1420\xi^3 \quad (\text{if } 0 \le \xi \le 1.0) \tag{13c}$$

$$K_{ts}/K_{t\mathrm{E}} = 1.148 - 0.160\eta - 0.0345\eta^2 + 0.0693\eta^3 \quad (\text{if } 0 \le \eta \le 1.0) \tag{13d}$$

$$\xi = \sqrt{t/\rho}, \quad \eta = \sqrt{\rho/t}, \quad K_{t\mathrm{E}} = 1 + \sqrt{t/\rho} \tag{13e}$$

$$K_{td}/K_{t\mathrm{H}} = 0.99744 + 0.014732x - 0.024870x^2 + 0.014924x^3 \tag{13f}$$

$$\begin{aligned} K_{t\mathrm{H}} &= (1/N)(3/4)(\sqrt{a/\rho + 1} \\ &+ 1)\left\{3(a/\rho) - (1 - 2\nu)\sqrt{a/\rho + 1} + 4 + \nu\right\}, \\ N &= 3(a/\rho + 1) + (1 + 4\nu)\sqrt{a/\rho + 1} \\ &+ (1 + \nu)/\left(\sqrt{a/\rho + 1} + 1\right) \end{aligned} \tag{13g}$$

Fig. 14 shows an example of a SCF chart obtained by the equations for torsion, tension and bending.

8. Conclusions

The stress concentration of a circumferential groove in a round bar is important for test specimens used to investigate fatigue strength of engineering materials under torsion, tension and bending. In this paper, the stress concentration formulas were considered for all notch shape. Here, the exact solutions now available for the limiting cases $2t/D \to 0,1$ were utilized together with accurate numerical results obtained by the body force method. The conclusions can be summarized as follows.

(1) The effect of notch opening angle on the stress concentration factor was considered for the limiting cases. The effect appears to be significant for the shallow notches under torsion, and for the deep notches under bending. It should be noted that for sharp and shallow notches under torsion the stress concentration varies depending on the notch opening angle ω and then the difference between the results of $\omega = 0$ and 90° is more than twice (see $t/\rho = 400$ in Fig. 3(a)).
(2) By the application of the body force method to the limiting cases of deep and shallow notches, accurate formulas were obtained as K_{td} and K_{ts} for the whole range of notch shape. However, the K_{ts} solution cannot be a good approximation for the stress concentration factor K_t under torsion compared to the cases of tension and bending. On the other hand, the K_{td} solution can be used as a good approximate formula compared to the cases of tension and bending.
(3) The notch shape can be classified into several groups according to the notch radius and notch depth. The least squares method can be applied for the calculation of K_t/K_{td}, and finally, a set of convenient formulas was proposed that is useful for any dimensions of notch in a round test specimen. The formulas give SCFs with less than 1% error for any shape of notch.

Acknowledgements

The authors wish to express their thanks to the members of their group, especially Yousuke ETOU, who carried out much of the constructional work.

References

[1] Noda N-A, Takase Y. Stress concentration formulas useful for any shape of notch in a round test specimen under tension and under bending. Fatigue Fract Eng Mater Struct 1999;22: 1071–82.
[2] Noda N-A, Takase Y. Stress concentration factor formulas useful for all notch shapes in a flat test specimen under tension and bending. J Test Eval 2002;30(5):369–81.
[3] Neuber H. Kerbspannungslehre. Berlin: Springer-Verlag; 1957.
[4] Kikukawa M, Sato Y. Stress concentration of a flat and round bar under tension and bending. Trans Jpn Soc Mech Eng 1985;38: 1663–87 (in Japanese).
[5] Nisitani H. The two-dimensional stress problem solved using an electric digital computer. Bull JSME 1968;11:14–23.
[6] Nisitani H. Solution of notch problems by body force method. Mechanics of Fracture, vol. 5. Noordhoff; 1978. p.1–68.
[7] Murakami Y, Noda N-A, Nisitani Y. Application of body force method to stress concentration of an axi-symmetric

body under bending, 3rd Report: V- and U-notch in a round bar under bending. Trans Jpn Soc Mech Eng 1982;48:800–9 (in Japanese).

[8] Nisitani H, Noda N-A. Study on the stress concentration problem of a cylindrical bar having a 60° V-shaped circumferential groove under tension. Trans Jpn Soc Mech Eng 1985;51:54–62 (in Japanese).

[9] Nisitani H, Noda N-A. Stress concentration of a cylindrical bar with a v-shaped circumferential groove under torsion, tension or bending. Eng Fract Mech 1984;20:743–66.

[10] Takase Y, Noda N-A, Gao Y, Takemoto T. Stress concentration formula useful for any dimensions of notches—Effect of notch opening angle on the stress concentration factor. J Soc Mater Sci Jpn 2003;52:795–800 (in Japanese).

[11] Noda N-A, Takase Y, Monda K. Stress concentration factors for round and flat test specimens with notches. Int J Fatigue 1995;17: 163–78.

[12] Noda N-A, Takase Y, Monda K. Stress concentration factors for round and flat test specimens with notches. Kikai no Kenkyu (Science of Machine) 1996;48(7):757–62 (in Japanese).

[13] Noda N-A, Takase Y. Generalized stress intensity factors of v-shaped notch in a round bar under torsion, tension, and bending. Eng Fract Mech 2003;70:1447–66.